Mechanism of formation of the MV$^{\bullet+}$ radical during the UV excitation of methylviologen

Erick E. Méndez[1], Carlos Crespo-Hernández, Roberto Figueroa,
Rafael Arce[2], Edwin Quiñones*

Department of Chemistry, University of Puerto Rico, PO Box 23346, San Juan 00931-3346, Puerto Rico

Abstract

The UV illumination of diluted aqueous solutions of methylviologen (MV^{2+}) leads to the formation of the methylviologen radical (MV$^{\bullet+}$), without the use of microheterogeneous materials or sacrificial electron donors. In the absence of O$_2$ the MV$^{\bullet+}$ radical remains in solution for hours. The formation mechanism of MV$^{\bullet+}$ was investigated employing the laser flash photolysis technique. The hydrated electron (e$_{aq}^-$) band and the characteristic bands of the MV$^{\bullet+}$ radical at 395 and 605 nm were detected in the MV^{2+} transient absorption spectra. This indicates that (1) MV^{2+} is ionized at 266 nm and (2) the e$_{aq}^-$ + MV^{2+} reaction is a source of the MV$^{\bullet+}$ radical. The rate constant for this reaction was measured at pH 6.5 to be $(3.8 \pm 0.1) \times 10^{10}$ M^{-1} s^{-1} and its magnitude is in good agreement with literature values. The ionization quantum yield of 0.16 was determined for MV^{2+} using KI as a reference actinometer. The photodestruction quantum yield of MV^{2+} was calculated to be $(8.7 \pm 0.5) \times 10^{-3}$ molecules/quantum. The formation quantum yield of MV$^{\bullet+}$ was measured at the two absorption maxima of the radical, ϕ (395 nm) = $(4.8 \pm 0.5) \times 10^{-3}$ and ϕ (605 nm) = $(5.1 \pm 0.3) \times 10^{-3}$ molecules/quantum. © 2001 Elsevier Science B.V. All rights reserved.

Keywords: Methylviologen radical; UV excitation; Quantum yield; Photodestruction

1. Introduction

The production of molecular hydrogen from water has long been recognized as an important process to solving our energetic needs [1–8]. To this end, the photosensitized reduction of MV^{2+} has been employed to generate the methylviologen radical, which cleaves water producing hydrogen in the presence of catalysts [9–15] Although the oxidative electronic quenching of a number of molecules leads to the formation of the MV$^{\bullet+}$ radical, the efficiency for producing hydrogen in homogeneous solutions is low due to the fast charge recombination reaction. However, significant progress has been made towards retarding the charge recombination employing microheterogeneous materials such as vesicles [16–21], micelles [20–25,37,38], zeolites [26–28], and cyclodextrins [29]. The challenge has been to produce the MV$^{\bullet+}$ radical using visible light.

McKellar and Turner [30] reported the formation of the MV$^{\bullet+}$ radical in their conventional flash photolysis study of MV^{2+}, irradiating with UV light. Likewise, Ebbesen and co-workers [31,32] observed the formation of MV$^{\bullet+}$ in the 337 nm laser flash photolysis of 0.1 M MV^{2+}, in the presence of 1 M NaCl. These authors postulated the reaction, MV^{2+}(Cl$^-$)$_2$ + $h\nu$ → MV$^{\bullet+}$ + (Cl$_2$)$^{\bullet-}$, as the source of MV$^{\bullet+}$. They reported the absorption band of the (Cl$_2$)$^{\bullet-}$ radical around the 350–370 nm region. According to Ebbesen's mechanism, the formation of MV$^{\bullet+}$ is instantaneous because the Cl$^-$ ions are in contact with the MV^{2+} molecules.

The following results are reported in this paper: (1) the ionization of MV^{2+} is inferred from the observation of the hydrated electron absorption band in the methylviologen transient absorption spectra, (2) the presence of the absorption bands at 395 and 605 nm in the transient spectra indicate the formation of the MV$^{\bullet+}$ radical, and (3) the formation of the MV$^{\bullet+}$ radical during the UV continuous irradiation of diluted solutions of MV^{2+}. The decay constant of e$_{aq}^-$, the rate constant for the e$_{aq}^-$ + MV^{2+} reaction, and the ionization quantum yield of MV^{2+} are also reported. In addition, we observed the evolution of a gas (which we believe is H$_2$) during the continuous UV

* Corresponding author. Tel.: +764-0000, ext. 4810;
fax: +787-759-6885.
E-mail address: edquinon@rrpac.upr.clu.edu (E. Quiñones).
[1] Grantee of the US Agency for International Development through CLASP II El Salvador training project.
[2] Co-corresponding author.

irradiation of solutions of MV^{2+} in the presence of colloidal PtO_2, without the use of microheterogeneous systems.

2. Results and discussion

2.1. Transient absorption spectra of methylviologen

The ground state absorption spectrum of MV^{2+} in water extends from 220 to 300 nm, with maximum at 257 nm and molar absorption coefficient of $1.4 \times 10^4 \, M^{-1} \, cm^{-1}$. The laser irradiation at 266 nm of an oxygen-free $6.9 \times 10^{-5} \, M$ MV^{2+} solution at pH 6.5 produces the transient absorption spectra displayed in Fig. 1. The broad absorption band of the hydrated electron is observed above 475 nm in the spectrum recorded at 0.56 μs after the laser pulse (Fig. 1(a)). This indicates that MV^{2+} is ionized, and this primary process is represented by Eq. (2). Only a 2% reduction in the initial absorbance at 257 nm of MV^{2+} was observed after 120 laser pulses and this demonstrates the photochemical stability of the solutions. For this reason it was not necessary to correct the transient spectra for photodestruction effects, although the samples were changed three times during the acquisition of each transient spectrum. The characteristic absorption bands of the $MV^{\bullet+}$ radical cation, with maxima at 395 and 605 nm, are displayed in the spectrum recorded 1.0 μs after the laser pulse (Fig. 1(b)) [4].

2.2. Kinetic analysis of the e_{aq}^- absorption

The decay kinetics of the hydrated electron was examined at 720 nm and a representative profile is presented in Fig. 2. The overlap between the absorption bands of $MV^{\bullet+}$ and e_{aq}^- is small at this wavelength. This particular time-resolved absorption at 720 nm represents the average of 30 laser pulses. From the first-order fit of the data, the hydrated electron decay constant was obtained $(4.1 \pm$
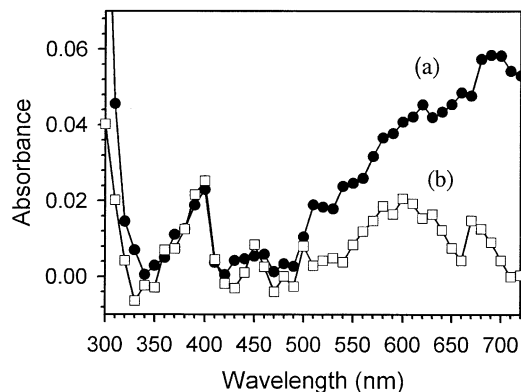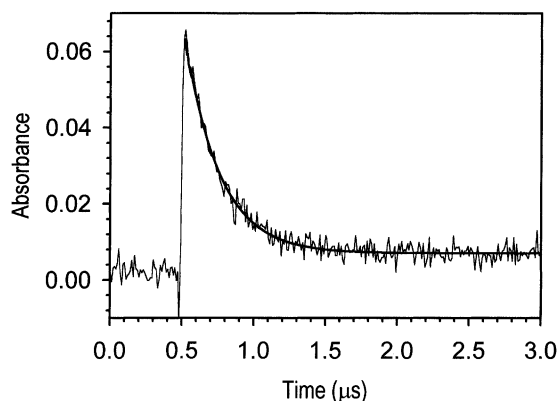

Fig. 2. Representative decay profile of the hydrated electron absorption at 720 nm after the laser photolysis at 266 nm. The methylviologen concentration, the pH, and the temperature of the solution were $6.9 \times 10^{-5} \, M$, 6.5, and 298 K, respectively. The decay constant of e_{aq}^- determined from this decay was, $k = (4.1 \pm 0.9) \times 10^{-5} \, s^{-1}$.

$0.9) \times 10^6 \, s^{-1}$. Note that under these conditions, e_{aq}^- is also being removed by the $e_{aq}^- + MV^{2+}$ reaction. Thus, we measured the decay of e_{aq}^- in pure water using a graphical method. A plot of the pseudo-first-order decay constants as a function $[MV^{2+}]$ gives a straight line (Fig. 3). The decay constant of e_{aq}^-, $k = (1.3 \pm 0.1) \times 10^6 \, s^{-1}$, was obtained from the intercept of this plot, whereas the rate constant for the $e_{aq}^- + MV^{2+}$ reaction was measured from the slope, $k_3(e_{aq}^- + MV^{2+}) = (3.8 \pm 0.1) \times 10^{10} \, M^{-1} \, s^{-1}$. The following kinetic scheme summarizes our observations:

$$MV^{2+} + h\nu \rightarrow (MV^{2+})^* \quad \text{(Electronic excitation)} \tag{1}$$

$$(MV^{2+})^* \rightarrow MV^{3+} + e_{aq}^- \quad \text{(Photoionization)} \tag{2}$$

$$MV^{2+} + e_{aq}^- \rightarrow MV^{\bullet+}$$
$$\text{(Formation of the } MV^{\bullet+} \text{ radical, } k_3) \tag{3}$$

Fig. 1. Room temperature transient absorption spectra of an aqueous solution $6.9 \times 10^{-5} \, M \, MV^{2+}$: (a) 0.56 μs after the laser pulse, and (b) 1.0 μs after the laser pulse. The solution was saturated with ultrapure $N_2(g)$ to remove O_2 and the pH was 6.5.
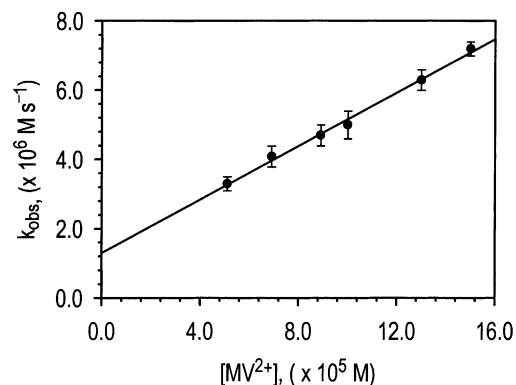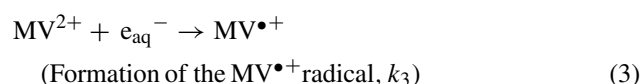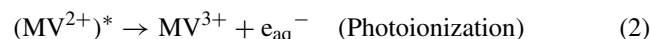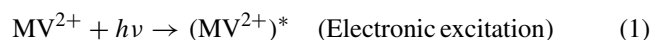

Fig. 3. Plot of the first-order decays of the electron against methylviologen concentration. An oxygen-free solution $6.9 \times 10^{-5} \, M \, MV^{2+}$ was examined. The slope of this plot gives the e_{aq}^- scavenging rate constant of MV^{2+}, $k_3(e_{aq}^- + MV^{2+}) = (3.8 \pm 0.1) \times 10^{10} \, M \, s^{-1}$, and the intercept the decay constant of e_{aq}^-, $k = (1.3 \pm 0.1) \times 10^6 \, s^{-1}$.

The value of k_3 at pH 6.5 is comparable to that obtained by Solar et al. [4] in alkaline pH, $7.5 \times 10^{10} \, M^{-1} \, s^{-1}$. Because there are no absorption bands in the transient spectra that could be assigned to MV^{3+} (formed through reaction 2), the fate of this species is unknown. However, our data indicates that the recombination reaction, $MV^{3+} + e_{aq}^-$, is not taking place. This tends to indicate that MV^{3+} is undergoing a very fast decomposition reaction, producing species unable to oxidize the $MV^{\bullet+}$ radical.

2.3. Mechanisms of formation of the $MV^{\bullet+}$ radical

A kinetic analysis of the $MV^{\bullet+}$ radical absorption at 395 nm is presented in Fig. 4. The absorption profile of the $MV^{\bullet+}$ radical (Fig. 4(a)) is observed from the photolysis of an O_2-free solution of MV^{2+}. The $MV^{\bullet+}$ absorption increases during the first microsecond after the laser pulse and it decays slowly afterwards. In contrast, when the solution is saturated with O_2, the initial slowly growing absorption is no longer observed and the signal decays faster (Fig. 4(b)). That is, even in the presence of oxygen the $MV^{\bullet+}$ radical is still being produced, its formation rate being instantaneous with respect to the response time of our spectrometer. Fig. 4(b) indicates that a process faster than reaction 3 is also producing $MV^{\bullet+}$. Thus, adding an electron scavenger such as O_2 it is possible to remove the hydrated electron from the solution, thereby suppressing reaction 3. Below we describe the experiments in which solutions saturated with O_2 ($[O_2] = 1.39 \times 10^{-3} \, M$) were irradiated. As we mentioned, oxygen acts as an electron scavenger,

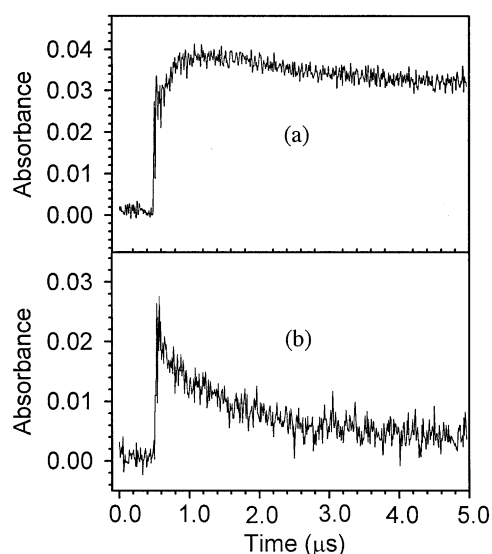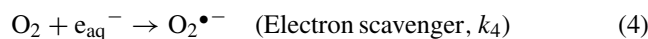$$O_2 + e_{aq}^- \rightarrow O_2^{\bullet-} \quad \text{(Electron scavenger, } k_4\text{)} \tag{4}$$

Fig. 4. Representative absorption time profiles of the $MV^{\bullet+}$ radical monitored at 395 nm after the 266 nm laser flash photolysis of an aqueous solutions of methylviologen: (a) oxygen-free solution, and (b) solution saturated with O_2 at 1 atm.

Note that the ratio of the rate of reactions 4 and 3 is independent of $[e_{aq}^-]$,

$$\frac{r_4}{r_3} = \frac{k_4[O_2]}{k_3[MV^{2+}]} \tag{5}$$

Using $k_3 = (3.8 \pm 0.1) \times 10^{10} \, M^{-1} \, s^{-1}$, $k_4(e_{aq}^- + O_2) = 1.88 \times 10^{10} \, M^{-1} \, s^{-1}$, $[O_2] = 1.39 \times 10^{-3} \, M$, and $[MV^{2+}] = 6.9 \times 10^{-5} \, M$, one obtains $r_4/r_3 \approx 10$. This result demonstrates that the slowly growing component in Fig. 4(b) is no longer observed because e_{aq}^- is removed by O_2. Further evidence of reaction 4 comes from the observation of a faster decay of the absorption of the hydrated electron at 720 nm when O_2 is present, as compared when an air-free solution is examined (data not shown). Reactions with O_2 has been implicated in the photodegradation of MV^{2+} [30].

Even though e_{aq}^- was removed by adding O_2, the instantaneous formation of $MV^{\bullet+}$ is still observed in Fig. 4(b). Clearly, reaction 3 is not the only formation route of $MV^{\bullet+}$. The kinetics of formation of $MV^{\bullet+}$ in the presence of O_2 can be explained using the mechanism postulated by Ebbesen and co-workers [31,32]. These authors observed the instantaneous formation of $MV^{\bullet+}$ since the Cl^- ion is the counter ion of MV^{2+} and they added a large concentration of the Cl^- ion. Note that the mechanism of Ebbesen et al. represents a static process while reaction 3 is a diffusion-controlled process. Although from a kinetic point of view the mechanism postulated by Ebbesen et al. is consistent with the kinetic data that we present in Fig. 4(b), the Cl^- concentrations in our experiments is much smaller than that employed by them.

Another possible mechanism of formation of $MV^{\bullet+}$ would be the electronic excitation of a MV^{2+} dimer, which can undergo an electron transfer reaction,

$$(MV^{2+})_2{}^* \rightarrow MV^{3+} + MV^{\bullet+} \tag{6}$$

Again, one has to assume that MV^{3+} decomposes very fast yielding products that cannot oxidize $MV^{\bullet+}$. However, the experimental data presented do not allow us to distinguish between these mechanisms.

2.4. Continuous illumination of solutions of MV^{2+}

The absorption spectra of the $MV^{\bullet+}$ radical that result from the low intensity irradiation of a solution $1.4 \times 10^{-4} \, M$ MV^{2+} are displayed in Fig. 5. The samples for this experiment were vacuum-sealed and the pH was 3.5. The two characteristic absorption bands of the $MV^{\bullet+}$ radical are observed at 395 and 605 nm [4,31,32]. In the inset of Fig. 5 is plotted the absorption at 395 nm of $MV^{\bullet+}$ as a function of irradiation time. The $MV^{\bullet+}$ absorption increases up to 60 min, but subsequently reaches a plateau. The samples are irradiated using a Corning 7-54 filter, which transmits from 220 to 460 nm. The transmittance at 395 nm is about 15%, but it increases rapidly below 400 nm. This means that $MV^{\bullet+}$ also
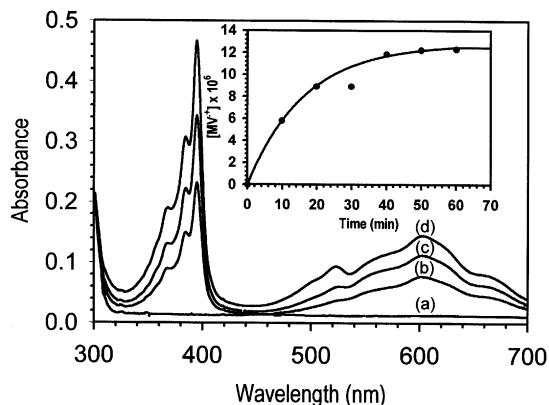
Fig. 5. Absorption spectra of the $MV^{\bullet+}$ radical in an oxygen-free solution at room temperature at the following irradiation times: (a) prior to irradiation, (b) 10 min, (c) 20 min, and (d) 60 min. The irradiation source was a 150 xenon lamp and $[MV^{2+}] = 1.39 \times 10^{-4}$ M. A Corning 7-54 filter and a water filter were placed in front of the sample. The inset shows the buildup of the $MV^{\bullet+}$ radical as a function of irradiation time.

Fig. 6. Plot of the absorbance measured for the hydrated electron against laser pulse energy for (a) a 71 μM MV^{2+} solution, and (b) a 0.16 M KI solution. KI is the reference system, which undergoes ionization through a monophotonic mechanism and it displays a linear behavior. Methylviologen exhibits a non-linear behavior indicating the participation of multiphoton pathways.

absorbs light (see Fig. 5) and for this reason the absorption reaches a steady-state condition.

When oxygen-free samples of MV^{2+} are irradiated using a low power Xe lamp in the presence of colloidal PtO_2, the continuous evolution of H_2 is observed [16,23]. The present system can be described as follows: (1) the $MV^{\bullet+}$ radical can be generated at room temperature by irradiating oxygen-free MV^{2+} solutions with a low intensity UV source, (2) the generation of a gas, which we believe is H_2, is vigorous, (3) it is possible to carry out spectroscopic studies of the $MV^{\bullet+}$ radical without the spectral interference of other molecules such as electron donors, and (4) reactions of $MV^{\bullet+}$ radical with other molecules can be studied in a vacuum line.

The formation of $H_2(g)$ was not confirmed directly. We observed that oxygen-free colloidal MV^{2+} solutions can be irradiated for an hour and the evolution of a colorless gas is still observed. In contrast, experiments in which we allowed oxygen to enter the photolysis cell did not show gas evolution. For this reason we know that O_2 is *not* the gas being evolved during the photolysis. The other possibility must be $H_2(g)$.

2.5. Concentration of e_{aq}^- against laser fluence

Fig. 6(a) displays the results of measurements of the absorbance of the hydrated electron at 720 nm for a solution 71 μM of MV^{2+} as a function of laser pulse energy. As a reference system, the behavior of a 0.16 M KI solution is also presented in Fig. 6(b). The KI solution is known to photoionize through a monophotonic mechanism [33,34]. All the data displayed in Fig. 6 was collected the same day using fresh samples. None of these systems exhibit saturation effects at the laser fluences examined in the present experiments. Each experiment was first performed measuring
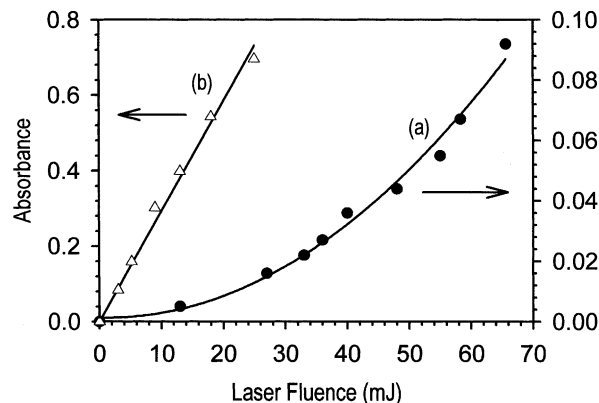
the absorbances at 720 nm increasing the laser fluence, and then repeated decreasing the laser fluence. The results in each case were almost identical. This procedure was followed to avoid errors due to laser fluence fluctuations. We first confirmed that the ionization of the I^- ion follows a monophotonic mechanism. A plot of $\log(A_{720})$ versus $\log(\text{laser fluence})$ gives a slope of 1.12, and the extrapolation of the line to zero laser fluence gives zero I^- concentration [33]. In the case of methylviologen, a plot of $\log(A_{720})$ versus $\log(\text{laser fluence})$ gives a slope of 1.5. The fact that the data displayed in Curve (a) cannot be fitted to a straight line tends to indicate that more than one photon are involved in the ionization of MV^{2+}. However, the plot of $\log(A_{720})$ versus $\log(\text{laser fluence})$ is not providing a definite answer.

2.6. Ionization quantum yield of MV^{2+}

The ionization quantum yield (Φ) of MV^{2+} was determined using KI as a reference system. Bryant et al. [34] determined $\Phi = 0.36$ for KI at 720 nm. We irradiated a solution 71 μM of MV^{2+} at the same laser fluence used in the KI experiments (i.e., 30 mJ) to obtain $\Phi \approx 0.16$ for methylviologen.

2.7. Formation quantum yield of $MV^{\bullet+}$

The formation quantum yield of the radical was determined following the procedure recently described by Crespo-Hernández et al. [36] irradiating a solution 9.6×10^{-5} M MV^{2+} at 253.7 nm with a low-intensity Hg lamp. Samples sealed under vacuum were irradiated during 5 min intervals. Concentration measurements of $MV^{\bullet+}$ and MV^{2+} were performed at different irradiation times using the following molar absorption coefficients: $\varepsilon(MV^{2+}, 257\,\text{nm}) = 1.4 \times 10^4\,\text{M}^{-1}\,\text{s}^{-1}$, $\varepsilon(MV^{\bullet+}, 395\,\text{nm}) = 3.8 \times 10^4\,\text{M}^{-1}\,\text{s}^{-1}$,

and $\varepsilon(MV^{\bullet+}, 605\,nm) = 1.1 \times 10^4\,M^{-1}\,s^{-1}$ [31]. From the absorption spectra (data not shown) it is observed a decrease of the MV^{2+} band with maximum at 257 nm with irradiation time and a simultaneous increase of the bands of $MV^{\bullet+}$ at 395 and 605 nm. The spectra present isosbestic points at 235 and 290 nm. The photodestruction yield of MV^{2+} was calculated to be $\phi(MV^{2+}) = (8.7 \pm 0.5) \times 10^{-3}$ molecules/quantum. On the other hand, the formation yield of the $MV^{\bullet+}$ radical was determined at two wavelengths, $\phi(MV^{\bullet+}, 395\,nm) = (4.8 \pm 0.5) \times 10^{-3}$ and $\phi(MV^{\bullet+}, 605\,nm) = (5.1 \pm 0.3) \times 10^{-3}$ molecules/quantum. The fact that the $\phi(MV^{\bullet+})$ determined at the two wavelengths are the same within the experimental error indicate that apart from $MV^{\bullet+}$ there is no other photoproduct absorbing at wavelengths longer than 300 nm (see Fig. 5). However, the fact that $\phi(MV^{2+})$ is larger than $\phi(MV^{\bullet+})$ suggests that other photoproducts are formed, although are not observed in the absorption spectra.

3. Experimental section

3.1. Methods and instruments

A general description of the laser flash spectrometer used in this work may be found elsewhere [35]. Briefly, the excitation was provided by a Q-switched Nd:YAG laser (Continuum Surelite II) delivering pulses with maximum energy of 70 mJ at 266 nm, with an energy fluctuation of less than 10%. The pulse energy was measured at the sample position using a Newport multifunction optical meter connected to a calorimeter (Newport, Mod. 8165-50). The laser beam was not focused. The laser time profile is Gaussian and the pulse duration is 6 ns. A 0.22 m Spex monochromator (Mod. 1680) was used to disperse the analysis light. The monochromator was coupled to a Hamamatsu R928 photomultiplier. Each data point in the transient absorption spectra corresponds to an average of five laser pulses. The signal was recorded using a digital oscilloscope (LeCroy 9360) and the data transfer and part of the analysis was done using Lab View, installed in a Pentium/300 MHz computer.

3.2. Continuous photolysis experiments

Vacuum-sealed samples of MV^{2+} were irradiated using a high pressure 150 W Xe Arc lamp (Oriel) to generate the $MV^{\bullet+}$ radical. A 10 cm water cell and a Corning 7-54 filter were placed in front of the photolysis cell.

3.3. Sample preparation

The samples were prepared using TOC-free water (Environment Science and Technology). The ground state absorption spectra were recorded using a Cary (model 219) spectrophotometer to confirm the purity of the samples and to determine their concentrations. Methylviologen dichloride (Aldrich) was re-crystallized from ethanol and the concentration of the solution was 0.1 g/4 ml [32]. PtO_2 (Aldrich) was used as received and concentrations of 0.1 mg/ml were used. For the continuous irradiation experiments, oxygen was removed from the samples using the freeze-pump-thaw method. The samples were cooled using an ice/water mixture and sealed in a 1 cm quartz cells to which a glass valve was adapted. For the laser flash photolysis, the samples were sealed using septa and O_2 was removed saturating the samples with ultrapure N_2 (Gas Products).

References

[1] A.J. Bard, M.A. Fox, Acc. Chem. Res. 28 (1995) 141, and references therein.
[2] E. Amouyal, Solar Energy Mater. Solar Cells 38 (1995) 249.
[3] M.Z. Hoffman, J. Phys. Chem. 92 (1988) 3458.
[4] S. Solar, W. Solar, N. Getoff, J. Holcman, K. Sehested, J. Chem. Soc., Faraday Trans. 78 (1982) 2467.
[5] Y. Amao, I. Okura, J. Mol. Catal. A 105 (1996) 125.
[6] J.R. Bolton, Solar Energy Mater. Solar Cells 38 (1995) 543.
[7] D.F. Katakis, C. Mitsopoulou, J. Konstantatos, E. Vrachnou, P. Falaras, J. Photochem. Photobiol. A 68 (1992) 375.
[8] M. Grätzel, Heterogeneous Photochemical Electron Transfer, CRC Press, Boca Raton, CA, 1989.
[9] X. Xu, K. Shreder, B. Iverson, A.J. Bard, J. Am. Chem. Soc. 118 (1996) 3656.
[10] M. Georgopoulos, M.Z. Hoffman, J. Phys. Chem. 95 (1991) 7717.
[11] P. Keller, A. Moradpour, J. Am. Chem. Soc. 102 (1980) 7193.
[12] S.F. Chan, M. Chou, C. Creutz, T. Matsubara, N. Sutin, J. Am. Chem. Soc. 103 (1981) 369.
[13] K. Yamaguchi, A. Kuwabara, H. Miyama, R. Baba, A. Fujishima, Y. Nosaka, J. Photochem. Photobiol. A 64 (1992) 375.
[14] I. Okura, Y. Kinumi, N. Kaji, S. Aono, J. Macromol. Sci. Chem. A 25 (1988) 1275.
[15] O. Johansen, A.W.H. Mau, H.F. Sasse, Chem. Phys. Lett. 94 (1983) 113.
[16] M.S. Tunuli, J.H. Fendler, J. Am. Chem. Soc. 103 (1981) 2507.
[17] S. Lukac, J.R. Harbour, J. Am. Chem. Soc. 105 (1983) 4248.
[18] W.E. Ford, J.W. Otvos, M. Calvin, Nature 274 (1978) 507.
[19] M. Aikawa, N.J. Turro, K. Ishiguro, Chem. Phys. Lett. 222 (1994) 197.
[20] S.M. Hubig, M.A.J. Rodgers, J. Phys. Chem. 94 (1990) 1933.
[21] E. Joselevich, I. Willner, J. Phys. Chem. 93 (1995) 6903.
[22] B. Claude-Montigny, A. Merlin, C. Tondre, J. Phys. Chem. 96 (1992) 4432.
[23] H.J.D. McManus, Y.S. Kang, L. Kevan, J. Phys. Chem. 96 (1992) 2274.

[24] M.J. Colaneri, L. Kevan, R. Schmehl, J. Phys. Chem. 93 (1989) 397.

[25] R. Schmehl, D.G. Whitten, J. Am. Chem. Soc. 102 (1980) 1938.

[26] K. Kalyanasundaram, Photochemistry in Microheterogeneous Systems, Academic Press, Orlando, FL, 1987.

[27] Y.I. Kim, S.W. Keller, J.S. Krueger, E.H. Yonemoto, G.B. Saupe, T.E. Mallouk, J. Phys. Chem. B 101 (1997) 2491.

[28] M. Alvaro, H. García, S. García, F. Márquez, J.C. Scaiano, J. Phys. Chem. B 101 (1997) 3043.

[29] J.W. Park, N.H. Choi, J.H. Kim, J. Phys. Chem. B 100 (1996) 769.

[30] J.F. McKellar, P.H. Turner, Photochem. Photobiol. 13 (1971) 437.

[31] T.W. Ebbesen, G. Levey, L.K. Patterson, Nature 298 (1982) 545.

[32] T.W. Ebbesen, G. Ferraudi, J. Phys. Chem. 87 (1983) 3717.

[33] U. Lachish, A. Shafferman, G. Stein, J. Chem. Phys. 64 (1976) 4205.

[34] D.F. Bryant, R. Santus, L.I. Grossweiner, J. Phys. Chem. 79 (1975) 2711.

[35] E. Quiñones, R. Arce, J. Am. Chem. Soc. 111 (1989) 8218.

[36] C.E. Crespo-Hernández, S. Flores, C. Torres, I. Negrón-Encarnación, R. Arce, Photochem. Photobiol. 71 (2000) 534.

[37] M.A.J. Rodgers, J.C. Becker, J. Phys. Chem. 84 (1980) 2762.

[38] M.A.J. Rodgers, D.C. Foyd, Z.A. Zimek, Radiat. Res. 75 (1978) 296.